

Singularities in gravitational collapse with radial pressure

Sérgio M. C. V. Gonçalves*

Theoretical Astrophysics, California Institute of Technology, Pasadena, California 91125

Sanjay Jhingan

Yukawa Institute for Theoretical Physics, Kyoto University, Kyoto 606-8502, Japan

October 30, 2018

Abstract

We analyze spherical dust collapse with non-vanishing radial pressure, Π , and vanishing tangential stresses. Considering a barotropic equation of state, $\Pi = \gamma\rho$, we obtain an analytical solution in closed form—which is exact for $\gamma = -1, 0$, and approximate otherwise—near the center of symmetry (where the curvature singularity forms). We study the formation, visibility, and curvature strength of singularities in the resulting spacetime. We find that visible, Tipler strong singularities can develop from generic initial data. Radial pressure alters the spectrum of possible endstates for collapse, increasing the parameter space region that contains no visible singularities, but *cannot* by itself prevent the formation of visible singularities for sufficiently low values of the energy density. Known results from pressureless dust are recovered in the $\gamma = 0$ limit.

Keywords: Gravitational collapse, singularities, black holes.

*E-mail: sergiog@its.caltech.edu, Tel: +1-626-395-8753, Fax: +1-626-796-5675

1 Introduction

It has long been known that under a variety of circumstances, spacetimes which are solutions of Einstein's equations with physically reasonable regular initial data, inevitably develop singularities [1]. These are events at which Riemannian curvature typically diverges, the spacetime is geodesically incomplete, and classical general relativity necessarily breaks down. The question of whether these singularities can be visible is one of the outstanding problems in general relativity.

In an effort to protect the applicability of general relativity, Penrose proposed that such singularities might be hidden by an event horizon, and thus invisible to an asymptotic observer, i.e., they cannot be *globally* naked [2]. This constitutes in essence what has become known as the *weak cosmic censorship conjecture*. However, it is quite possible—at least in principle—for an observer to penetrate the event horizon and live a rather normal life inside a black hole. This motivated the *strong cosmic censorship conjecture*, which broadly states that timelike singularities cannot occur in nature, i.e., they cannot be visible even *locally* [3].

A lack of tools to handle global properties of the Einstein equations (and respective solutions), together with their high non-linearity, have been the main obstacle to provable formulations of either form of the cosmic censorship conjecture. Whilst efforts are being undertaken in this direction [4], one can hope that the detailed study of specific models helps to isolate some defining features of singularity formation and structure, thereby contributing towards a precise, counter-example-free formulation of the conjecture.

One such model is Lemaître-Tolman-Bondi (LTB) [5] inhomogeneous dust collapse, whose general solution is analytically obtainable in closed (or parametric) form. The exact solvability of this model has resulted in many detailed studies by various authors [6, 7]. These analyses show that, from generic initial data, a null (central) singularity develops, which is Tipler strong [8], and can be locally or globally naked, depending on the differentiability of the initial density profile at the center [9]. In addition, the singularity is stable against initial density perturbations [10], and marginally stable against linear non-spherical perturbations [11]. It is fair to say that singularity formation and structure in LTB collapse are now very well understood.

Whilst spherical symmetry may, arguably, constitute a reasonable approximation to realistic collapse [12], pressureless dust evidently fails to be a realistic form of matter, especially at the late stages of stellar collapse, where an effective equation of state must be considered, and radial and tangential stresses come into play [13]. The inclusion of pressure has been studied analytically in the perfect fluid

and anisotropic pressure cases; the former, when self-similarity [14, 15], or special equations of state [16] are assumed.

Early analytical studies of perfect fluid collapse were restricted to approximate solutions of Einstein’s equations near the singularity [17]. This technique was generalized to include a barotropic equation of state, $p = k\rho$, for perfect fluids, but the results were restricted to the analysis of non-central shells due to simplifying assumptions [18]. Numerical studies of self-similar [19] and perfect fluid collapse with barotropic equation of state [20] have shown the formation of a central visible (globally naked, in the self-similar case) singularity. The work of Joshi and Dwivedi [21] showed the possibility of naked singularity formation in the collapse of general “type I” matter fields [22], but their analysis does not provide an explicit relation between the initial data—such as densities and pressures—and the conditions for formation of visible singularities; (such a relation is very clear in the LTB case).

Recently, models with only tangential stresses have been analyzed. In particular, the Einstein cluster class is now completely understood [23]. Tangential stresses tend to uncover part of the singularity spectrum, thereby showing that the role of tangential stresses is not negligible, and lending support to the idea that naked singularities develop from generic gravitational collapse [24].

In this paper, we present an new solution of spherical dust collapse with non-vanishing radial pressure, and vanishing tangential stresses. This solution is exact for $\gamma = -1$ and $\gamma = 0$. For other values of $\gamma \in (-1, 1)$, it asymptotes the exact solution in the $r = 0$ limit, which is the region of interest, where the curvature singularity forms. In particular, the solution can be made to obey Einstein’s equations to arbitrarily small error, by considering an arbitrarily small neighborhood of the $r = 0$. In this way, the role of radial pressure—as opposed to the combined contribution of radial and tangential stresses, as in the perfect fluid case—is isolated and its effects on singularity formation and structure become clear. For configurations with radial pressure Π linearly proportional to the density ($\Pi = \gamma\rho$), that can end up in either a black hole or naked singularity, an increase in radial pressure leads to a decrease in the parameter space area for naked singularities. In the initial two-parameter data space (radial pressure vs. density), visible singularities are shown to exist for the entire range of the adiabatic index γ . This shows that, whereas radial pressure can cover singularities that would otherwise be visible, it cannot, by itself prevent the formation of visible singularities.

This paper is organized as follows. In Sec. II, Einstein’s equations are solved for a spherically symmetric system with non-vanishing radial pressure. The ansatz of marginally bound configurations yields a complete analytical treatment in closed form. In Sec. III, conditions for singularity formation are discussed. Section IV studies the visibility of the central curvature singularity and discusses the

role of radial pressure. Curvature strength is computed in Sec. V. Section VI discusses the pure dust limit ($\gamma = 0$) of our model. Section VII concludes with a summary and discussion.

Geometrized units, in which $G = c = 1$, are used throughout.

2 Spherically symmetric collapse with radial pressure

We consider a general spherically symmetric metric, in standard spherical coordinates $\{t, r, \theta, \phi\}$:

$$ds^2 = -e^{2\Phi(t,r)} dt^2 + e^{-2\Psi(t,r)} dr^2 + R^2(t,r) d\Omega^2, \quad (1)$$

where $R(t, r)$ is the proper area radius and $d\Omega^2 = d\theta^2 + \sin^2 \theta d\phi^2$ is the canonical metric of the unit two-sphere.

The stress-energy tensor is:

$$T_a^b = \text{diag}(-\rho, \Pi, \Sigma, \Sigma) \quad (2)$$

where ρ , Π , and Σ are the energy density, radial pressure, and tangential stress, respectively.

With the metric (1) the non-vanishing Einstein tensor components are:

$$G_{tt} = \frac{e^{2(\Psi+\Phi)}}{R^2} [2R(R'' + R'\Psi') + R'^2 - e^{-2\Psi}] - \frac{\dot{R}}{R} \dot{\Psi} + \left(\frac{\dot{R}}{R}\right)^2, \quad (3)$$

$$G_{tr} = \frac{2}{R} (\dot{R}' - \dot{R}\Phi' + \dot{\Psi}R'), \quad (4)$$

$$G_{rr} = \frac{e^{-2(\Psi+\Phi)}}{R^2} [2R(\dot{R}\dot{\Phi} - \ddot{R}) - \dot{R}^2 - e^{2\Psi}] + \frac{R'}{R^2} (R' + 2R\Phi'), \quad (5)$$

$$G_{\theta\theta} = -R^2 \left\{ e^{-2\Phi} \left[-\frac{\dot{R}}{R} (\dot{\Phi} + \dot{\Psi}) + \frac{\ddot{R}}{R} + \dot{\Psi}^2 - \ddot{\Psi} + \dot{\Phi}\dot{\Psi} \right] - e^{2\Psi} \left[\frac{R'}{R} (\Phi' + \Psi') + \frac{R''}{R} + \Phi'^2 + \Phi'' + \Phi'\Psi' \right] \right\}, \quad (6)$$

$$G_{\phi\phi} = \sin^2 \theta G_{\theta\theta}, \quad (7)$$

where $' \equiv \partial_r$ and $\dot{} \equiv \partial_t$.

Introducing the auxiliary functions

$$k(t, r) \equiv 1 - e^{2\Psi} R'^2, \quad (8)$$

$$m(t, r) \equiv \frac{1}{2} R (e^{-2\Phi} \dot{R}^2 + k), \quad (9)$$

Einstein's equations can be recast as

$$m' = 4\pi R^2 R' \rho, \quad (10)$$

$$\dot{m} = -4\pi R^2 \dot{R} \Pi, \quad (11)$$

$$\Phi' = (\rho + \Pi)^{-1} \left[2 \frac{R'}{R} (\Sigma - \Pi) - \Pi' \right], \quad (12)$$

$$\dot{\Psi} = \frac{\dot{R}}{R'} \Phi' - \frac{\dot{R}'}{R'}. \quad (13)$$

Note that the function $m(t, r)$ is just the Misner-Sharp mass [25]:

$$m(t, r) = \frac{R}{2} (1 - R_{,a} R_{,b} g^{ab}). \quad (14)$$

It then follows that the function $k(t, r)$ is the binding energy per unit mass of a shell r , with area radius $R(t, r)$. Gravitationally bound configurations have $0 < k < 1$; unbound configurations have $k < 0$, and $k = 0$ corresponds to the marginally bound case.

From Eq. (9), an “acceleration” equation for the area radius can be easily obtained:

$$\ddot{R} = \dot{\Phi} \dot{R} - e^{2\Phi} \left[4\pi \Pi R + \frac{m}{R^2} + (k - 1) \frac{\Phi'}{R'} \right]. \quad (15)$$

When the tangential stresses vanish, $\Sigma = 0$, Eq. (12) simplifies to:

$$\Phi' = -(\rho + \Pi)^{-1} \left(2 \frac{R'}{R} \Pi + \Pi' \right). \quad (16)$$

2.1 Marginally bound models

Let us consider the case $k = 0$, corresponding to marginally bound configurations. From Eq. (8), provided $R' > 0$ (i.e., absence of shell-crossings), it follows that

$$\dot{\Psi} = -\frac{\dot{R}'}{R'}, \quad (17)$$

which implies, from Eq. (13),

$$\Phi' = 0, \quad (18)$$

i.e., $\Phi = \Phi(t)$.

We obtain a closed system by specifying an equation of state, which we take to be of barotropic form:

$$\Pi = \gamma \rho, \quad (19)$$

where causality requires $\gamma^2 < 1$. From Eqs. (16) and (18) it follows that

$$\rho(t, r) = \frac{\omega(t)}{R^2(t, r)}, \quad (20)$$

where $\omega(t)$ is an arbitrary real-valued function of r .

Equations (10)-(11) now read

$$m' = 4\pi \omega R', \quad (21)$$

$$\dot{m} = -4\pi \omega \gamma \dot{R}. \quad (22)$$

Equation (21) readily integrates to

$$m(t, r) = 4\pi\omega R, \quad (23)$$

where the “constant” of integration (a function of t alone) was set to zero by demanding regularity at the center. Taking the partial time derivative of the above equation and equating it to Eq. (22) gives

$$\dot{\omega}R + (1 + \gamma)\omega\dot{R} = 0. \quad (24)$$

Which integrates to

$$\omega(t) = \omega_0(r)R^{-1-\gamma}, \quad (25)$$

where $\omega_0(r)$ is an integration “constant”, which can be fixed as $\omega_0(r) = Cr^{1+\gamma}$, by the choice $R(0, r) = r$, where $C \geq 0$. Hence,

$$\omega(t) = C \left(\frac{r}{R} \right)^{1+\gamma}. \quad (26)$$

From Eq. (19) we then have

$$\Pi(t, r) = \frac{\gamma C}{R^2} \left(\frac{r}{R} \right)^{1+\gamma}. \quad (27)$$

Note that C characterizes the “strength” of the initial density profile—which is, by construction, positive definite, thus enforcing the weak energy condition—whereas $\gamma \in (-1, 1)$ characterizes the relative strength of the radial pressure (which can be negative). If we regard Π as a hydrostatic pressure, then $\sqrt{\gamma}$ is the sound speed, which is complex for negative pressures. Since we do not know how matter behaves in high density regimes, such as the strong field regions surrounding the central singularity, we allow γ to be negative, within the limits imposed by the weak energy condition:

$$\rho + \Pi \geq 0 \Rightarrow \gamma \geq -1. \quad (28)$$

(Note that causality implies that this inequality does not saturate).

The mass function becomes

$$m(t, r) = 4\pi C R \left(\frac{r}{R} \right)^{1+\gamma}, \quad (29)$$

and the evolution equation simplifies to

$$e^{-2\Phi} \dot{R}^2 = 8\pi C \left(\frac{r}{R} \right)^{1+\gamma}. \quad (30)$$

Now, since $\Phi = \Phi(t)$, one can trivially rescale the comoving time t to proper time τ , via

$$d\tau = e^{\Phi(t)} dt \Rightarrow \tau = \int e^{\Phi(t)} dt + f(r). \quad (31)$$

Setting $f(r) = 0$, Eq. (30) becomes

$$\dot{R}^2(\tau, r) = 8\pi C \left(\frac{r}{R} \right)^{1+\gamma}, \quad (32)$$

where the dot denotes partial differentiation with respect to τ , and R is to be regarded as a function of the independent coordinates τ and r . Equation (32) integrates to

$$R(\tau, r) = A^{\frac{1}{3+\gamma}} r^{\frac{1+\gamma}{3+\gamma}} [\tau_0(r) - \tau]^{\frac{2}{3+\gamma}}, \quad (33)$$

where

$$A \equiv 2\pi C(3 + \gamma)^2, \quad (34)$$

and $\tau_0(r)$ is the proper time for complete collapse of a shell with area radius $R(0, r) = r$, which is given by

$$\tau_0(r) = \frac{r}{\sqrt{A}}. \quad (35)$$

Note that $\tau'_0 > 0$, for $r > 0$, which is a sufficient condition for the absence of shell-crossing singularities.

2.2 Approximate nature of the solution

A direct computation shows that Eq. (33) satisfies the Einstein equations exactly if $\gamma = 0$, or $\gamma = -1$. For other values of $\gamma \in (-1, 1)$, the $G_{\theta\theta}$ component of the field equations does not vanish identically. This arises because of the rescaling from t to τ , where an unknown function of r was arbitrarily set to zero, to render τ and r independent coordinates. This lack of exact solvability of the $G_{\theta\theta}$ component of the field equations is not detrimental, and can be made precise since

$$G_{\theta\theta} \propto (1 + \gamma)\gamma r^{2(1+\gamma)/(3+\gamma)} F(t, r), \quad (36)$$

where $F(t, 0) \propto t^{-(5+3\gamma)/(3+\gamma)}$. Since $\gamma \in (-1, 1)$, $G_{\theta\theta}$ is a monotonically increasing function of r , which can be made arbitrarily close to zero by considering an arbitrarily small neighborhood of $r = 0$, which is precisely the worldline of the central singularity. Therefore, by restricting ourselves to the vicinity of $r = 0$, Einstein's equations are satisfied to an arbitrarily small error in the region of interest.

Thus, although not an exact solution for general γ , our solution satisfies Einstein's equations to arbitrary precision, and, because it has the correct (exact) limiting behavior for $\gamma = -1$ and $\gamma = 0$, it provides a reliable test-bed for the study of the role of radial pressure in gravitational collapse. In addition to being an exact solution for $\gamma = -1, 0$, Eq. (33) captures all the relevant features of well-posed dust collapse for $\gamma \in (-1, 1)$: implosion, satisfaction of the weak energy condition, regular initial metric, and trapped-surface-free initial slice. Another example of a test-bed metric that is not an exact solution of Einstein's equations, but is useful for its physical content, is the Thorne test-bed metric for inspiralling binaries [26]. Such non-exact solutions are quite valuable in giving analytical, if qualitative, insights into physics that otherwise could only be explored numerically.

3 Conditions for singularity formation and visibility

The Kretschmann curvature scalar, $\mathcal{K} \equiv R_{abcd}R^{abcd}$, is

$$\mathcal{K} = 448\pi^2 C^2 \frac{1}{R^4} \left(\frac{r}{R}\right)^{2(1+\gamma)}, \quad (37)$$

which diverges at $R = 0$, thereby signaling the existence of a curvature singularity at a time τ_0 , where $R(\tau_0, r) = 0$. Choosing initial data with $\dot{R}(\tau_1, r) < 0$ [note that the choice $k = 0$ precludes the $\tau = 0$ slice from being a moment of time-symmetry, with $\dot{R}(0, r) = 0$], a sufficient condition for collapse is $\ddot{R}(\tau, r) \leq 0$, for $\tau_1 \leq \tau \leq \tau_0$. From Eq. (32), we have

$$\ddot{R}(\tau, r) = -\frac{4\pi C}{r}(1+\gamma) \left(\frac{r}{R}\right)^{2+\gamma}. \quad (38)$$

Hence, the condition for complete collapse of a shell r is

$$\gamma \geq -1, \quad (39)$$

which is always satisfied. Hence, provided $\dot{R}(\tau_1 < 0, r) < 0$, implosion always occurs, and the formation of a central curvature singularity is inevitable. Physically, our model corresponds to the initial radial pressure profile

$$\Pi(\tau_1, r) = \gamma C \left[\frac{r^{1+\gamma}}{R^{3+\gamma}} \right]_{\tau=\tau_1} < \frac{\gamma C}{r^2} = \Pi(0, r). \quad (40)$$

As collapse proceeds, Π becomes larger ($\dot{\Pi} > 0$), but the pressure build-up is never enough to halt collapse ($\ddot{R} < 0$). To this extent, this model is particularly useful for examining central curvature singularities—they always form.

In order to study the collapse of a finite spherical body, we have to introduce a cut-off at some finite coordinate radius r_c , and match the solution along the timelike three-surface $\Sigma_c : \{r = r_c\}$ thus defined to a Schwarzschild exterior. Formally, this is achieved by imposing the standard Darmois-Israel junction conditions [27] to enforce continuity of the metric and extrinsic curvature along Σ_c . Since our main focus is the central singularity and its properties, we shall not go into the details of the matching and dynamics of the junction surface; rather, we present qualitative arguments to show that such matching can be achieved and that it does not affect the behavior of the solution in the vicinity of the singularity. First, we note that the pressure falls off as r^{-2} , and thus we can consider a sufficiently large r_c , such that $\Pi(\tau, r_c) \ll 1$ (in appropriate mass-type units). If the cut-off at r_c is sharp (e.g. step-function), one of the components of the extrinsic curvature will fail to be C^0 on Σ_c . This can be remedied by considering a thin shell of matter, $r \in (r_c, r_c + \epsilon)$, where the radial pressure (hence the density) decreases smoothly from r_c to $r_c + \epsilon$, where it vanishes. In this case, the matching with a Schwarzschild exterior

is trivial at $r_c + \epsilon$, and one only needs to be concerned with the influence of the thin shell on the central singularity. This thin shell can be thought of as a perturbation that travels at the local sound speed $\sqrt{\gamma}$ [19]. Hence, provided we choose $r_c \gtrsim \mathcal{O}(\sqrt{\gamma}\tau_i)$, any hydrodynamic perturbations will arrive at the center *after* the singularity has formed. In addition, from a causal viewpoint, the existence of the thin shell will only introduce a discontinuity on the AH, when the latter crosses the worldline of r_c —the AH effectively “jumps out”—collapsing afterwards to the central singularity.

3.1 Apparent horizon

The singularity curve is given by Eq. (35). The evolution of the apparent horizon can give insight into the causal structure near the singularity. In the adopted spherical coordinates, the apparent horizon (AH), which is the outer boundary of a region containing trapped surfaces, is given by $2m(\tau_{\text{ah}}(r), r) = R(\tau_{\text{ah}}(r), r)$. This, from Eqs. (29) and (33), gives

$$\tau_{\text{ah}}(r) = \tau_0(r) \left[1 - \Theta^{(3+\gamma)/(1+\gamma)} \right], \quad (41)$$

with

$$\Theta \equiv \sqrt{8\pi C}, \quad (42)$$

where the exponent $(3 + \gamma)/(1 + \gamma) \in (2, +\infty)$, for $-1 < \gamma < 1$.

For non-central shells, the mass function $m(\tau, r)$ is positive definite and finite on any regular surface and, from Eq. (22), increasing afterwards ($\dot{m} > 0$). Therefore, for collapsing configurations, the quantity $2m/R$ increases monotonically, from its initial value (less than unity, which is the condition for non-existence of trapped surfaces for regular initial data), through unity (whence becoming trapped), before diverging positively at the singular surface, $\tau = \tau_0(r)$. The condition for absence of trapped surfaces on a given initial slice, $2m/R < 1$ on any $\tau_i < 0$ hypersurface, reads

$$\frac{2m}{R} = 8\pi C \left(\frac{r}{R} \right)^{1+\gamma} < 1. \quad (43)$$

Since $(r/R)^{1+\gamma} < 1$, $\forall \tau_i < 0$ and $\gamma > -1$, the above condition is satisfied provided

$$8\pi C \leq 1, \quad (44)$$

with strict inequality for the $\gamma = -1$ limiting case. Thus, we have $\tau_{\text{ah}}(r) \leq \tau_0$, where the inequality saturates for $r = 0$. Therefore, as expected, non-central shells are strongly censored and the singularity cannot be visible even locally. Only the central $r = 0$ singularity can be naked. Accordingly, we shall hereafter discuss the central ($r = 0$) singularity only.

4 Visibility

To show that a singularity is (at least locally) naked, one has to show the existence of non-spacelike future-directed outgoing geodesics with their past endpoint at the singularity. In geometric terms, this is equivalent to requiring that the area radius increases along such geodesics, i.e., $(dR/dr)_{\text{ORNG}} > 0$.

The equation for radial null geodesics (RNGs) is

$$\begin{aligned} \left(\frac{d\tau}{dr}\right)_{\text{RNG}} &= \pm R' \\ &= \pm \frac{R}{r} \frac{1}{3+\gamma} \left[1 + \gamma + 2 \left(1 - \frac{\tau}{\tau_0} \right)^{-1} \right], \end{aligned} \quad (45)$$

where the plus or minus sign corresponds to outgoing or ingoing RNGs, respectively. Along outgoing RNGs we have

$$\frac{dR}{dr} = R' + \dot{R} \left(\frac{d\tau}{dr} \right)_{\text{ORNG}} = R'(1 + \dot{R}). \quad (46)$$

Using the standard procedure [29], we introduce the auxiliary variables u , X :

$$u \equiv r^\alpha, \quad \alpha > 0, \quad (47)$$

$$X \equiv \frac{R}{u}. \quad (48)$$

In the limit of approach to the singularity we have

$$\begin{aligned} X_0 &\equiv \lim_{R \rightarrow 0, u \rightarrow 0} \frac{R}{u} = \lim_{R \rightarrow 0, u \rightarrow 0} \frac{dR}{du} \\ &= \lim_{R \rightarrow 0, r \rightarrow 0} \frac{1}{\alpha r^{\alpha-1}} \frac{dR}{dr} \\ &= \lim_{R \rightarrow 0, r \rightarrow 0} \frac{1}{\alpha r^{\alpha-1}} R'(1 + \dot{R}). \end{aligned} \quad (49)$$

X_0 is the value of the tangent to the geodesic on the $\{u, X\}$ plane, at the singularity. If $X_0 \in \mathbb{R}^+$, the singularity is at least locally naked, and covered otherwise. Now, from Eq. (33) we have

$$\tau(R, r) = \frac{r}{\sqrt{A}} \left[1 - \left(\frac{R}{r} \right)^{\frac{3+\gamma}{2}} \right], \quad (50)$$

and

$$R'(R, r) = \frac{R}{r(3+\gamma)} \left[1 + \gamma + 2 \left(\frac{r}{R} \right)^{\frac{3+\gamma}{2}} \right]. \quad (51)$$

Hence, near the singularity, $\tau_0(0)$, we obtain

$$\begin{aligned} X_0 &= \lim_{r \rightarrow 0} \frac{X}{\alpha(3+\gamma)} \left[1 + \gamma + 2 \frac{r^{(1-\alpha)(3+\gamma)/2}}{X^{(3+\gamma)/2}} \right] \times \\ &\quad \left[1 - \Theta \frac{r^{(1-\alpha)(1+\gamma)/2}}{X^{(1+\gamma)/2}} \right]. \end{aligned} \quad (52)$$

Clearly, for X_0 to be finite at $r = 0$ we must have $\alpha \leq 1$, since $\gamma \in (-1, 1)$. However, if $0 < \alpha < 1$, X vanishes identically on the $\tau = 0$ surface; hence, we must have $\alpha = 1$, such that X_0 is positive definite on the singular surface.

A self-consistent solution exists if $\alpha = 1$. In this case, the visibility of the singularity depends on the existence of positive roots of the equation

$$X_0^{2+\gamma} + \frac{1+\gamma}{2}\Theta X_0^{(3+\gamma)/2} - X_0^{(1+\gamma)/2} + \Theta = 0. \quad (53)$$

Since $-1 < \gamma < 1$, this algebraic equation is not a polynomial, and thus solutions cannot in general be found analytically. We note, however, the formal similarity with the corresponding equation for the general spherically symmetric dust case, where only the lowest-order term appears with a negative coefficient [9].

Even though the existence of real positive roots cannot be determined for general γ , one can analytically examine a sufficiently general class of initial data and draw conclusions from it. Take $\gamma \in [0, 1)$ and consider a class of initial data given by arbitrary C [subject to the constraint (44)] and $\gamma = 1/(2n)$, where $n \in \mathbb{N}^+ \setminus \{1\}$. The subset of initial data thus constructed is countable and infinite-dimensional, and hence physically significant. Equation (53) can then be rewritten as

$$Z^{4n+1} + \frac{2n+1}{4n}\Theta Z^{(6n+1)/2} - Z^{(2n+1)/2} + \Theta = 0, \quad (54)$$

$$Z \equiv X_0^{1/(2n)}. \quad (55)$$

This is a polynomial of odd-degree and hence it has at least one real root. Now, since $6n+1$ and $2n+1$ are odd, the second and third terms contain *ostensively* the square-root of Z . It then follows that the real solution(s) must be positive. For this class of initial data there always exists at least one positive real root of Eq. (53), and the central singularity is therefore at least locally naked. An analogous analysis for $\gamma \in (-1, 0]$ yields the same results.

A full numerical evaluation of all the real positive roots of Eq. (53) is shown in Fig. 1, which covers the entire initial data space, $\{\Theta \in (0, 1]\} \otimes \{\gamma \in (-1, 1)\}$.

It is instructive to examine the following special cases analytically, as they represent the maximum positive, negative, and zero pressure cases, respectively.

The limiting case $\gamma = 1$ reduces to the cubic polynomial:

$$Z^3 + \Theta Z^2 - Z + \Theta = 0, \quad (56)$$

whose solutions are trivial to analyze, for a given Θ . Standard methods from polynomial theory show that there is a critical value $\Theta_{\max} = 0.300283$, above which there are no positive real solutions. For

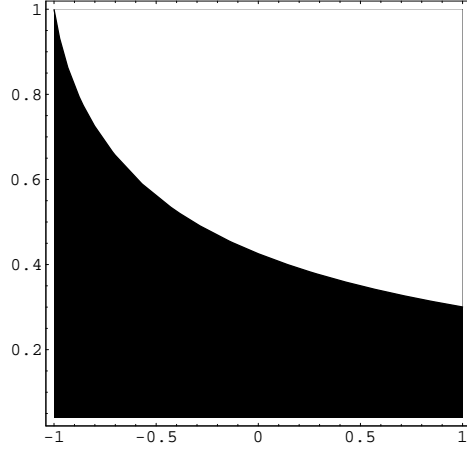


Figure 1: Parameter space for the occurrence of naked singularities. The density increases along the vertical axis (Θ), and radial pressure along the horizontal axis (γ). The shaded region corresponds to configurations that collapse to a visible singularity. Configurations with initial parameters in the white region end up in black holes and contain only spacelike singularities.

$0 \leq \Theta < \Theta_{\max}$, there are three real roots, two of which are positive. This case corresponds to the stiffest equation of state allowed. Even in such a case, visible singularities occur.

The case $\gamma = -1$ is trivial:

$$X_0 = 1 - \Theta \geq 0. \quad (57)$$

Hence, the singularity is always visible, since in this case $\Theta < 1$. This is consistent with the notion that negative radial pressure can lead to visible singularities that would otherwise be covered [18].

The $\gamma = 0$ case corresponds to a subclass of general inhomogeneous dust models [28], and will be dealt with separately in Sec. VI.

There are three relevant regions in the parameter space, defined by critical values of the strength of the initial density profile, Θ (or, equivalently, C):

Region I: $\Theta > 0.425343$. In this region all the singularities are covered, for positive values of the radial pressure. Collapse always ends up in a black hole covering a spacelike singularity, for $\gamma > 0$ and $\Theta > 0.425343$. For negative values of the radial pressure, both black holes and naked singularities can form. In the $\gamma = -1$ limit, collapse always leads to a visible central singularity. The more negative the pressure, the larger the number of configurations ending up in naked singularities.

Region II: $0.425343 \leq \Theta \leq 0.300283$. For negative pressure, collapse always ends up in a visible singularity. For positive pressure, there is a critical value, Θ_c , below which singularities are visible. When the radial pressure is sufficiently large ($\Theta > \Theta_c$), the singularities are strongly censored and

a black hole is the only final state of collapse. This is in marked contrast with what happens with tangential stresses, which tend to uncover the singularity.

Region III: $\Theta < 0.300283$. Collapse always leads to a visible singularity, irrespective of the radial pressure. In this case, the magnitude of the radial pressure is bounded from above, and it is not enough to censor the singularity. This region shows that radial pressure alone cannot rule out naked singularities.

4.1 Existence of an infinite number of ORNGs

Each real positive root of Eq. (53) uniquely defines an ORNG with past endpoint at the singularity, and a definite tangent value on the $\{u, X\}$ plane. To examine the possibility of a *family* of ORNGs emanating from the singularity, we briefly describe the method of Joshi and Dwivedi [29] and refer the reader to the original reference for further details.

Let us consider the ORNG equation on the $\{u, X\}$ plane:

$$\frac{dX}{du} = \frac{1}{u} \left(\frac{dR}{du} - X \right) = \frac{1}{u} [U(X, u) - X], \quad (58)$$

where

$$X_0 = \lim_{R \rightarrow 0, u \rightarrow 0} \frac{R}{u} = \lim_{R \rightarrow 0, u \rightarrow 0} U(X, u).$$

Now, let us rewrite the algebraic Eq. (53) as

$$V(X_0) \equiv (X_0 - X_0^*)(f_0 - 1) + f(X_0) = 0, \quad (59)$$

where X_0^* is one of the real positive roots, f_0 is a constant, and the function $f(X_0)$ contains higher-order terms in $(X_0 - X_0^*)$. We have then

$$\frac{dX_0}{du} = \frac{1}{u} [(X_0 - X_0^*)(f_0 - 1) + S], \quad (60)$$

where $S(X, u) \equiv U(X, u) - U(X, 0) + h(X_0)$ vanishes at the singularity. Using the integrating factor u^{1-f_0} , Eq. (60) integrates to

$$X_0 = X_0^* + Bu^{f_0-1} + u^{f_0-1} \int Su^{-f_0} du, \quad (61)$$

where B is a constant of integration that labels different geodesics. The last term always vanishes in the limit of approach to the singularity ($u \rightarrow 0$), independently of f_0 . Clearly, if $f_0 < 1$, the second term diverges, unless $B = 0$, which is required by the existence of the root X_0^* . In this case, a single ORNG departs from the singularity. However, if $f_0 > 1$, the second term always vanishes at the singularity, irrespective of B , and thus an infinite number of ORNGs (parameterized by B) departs from the

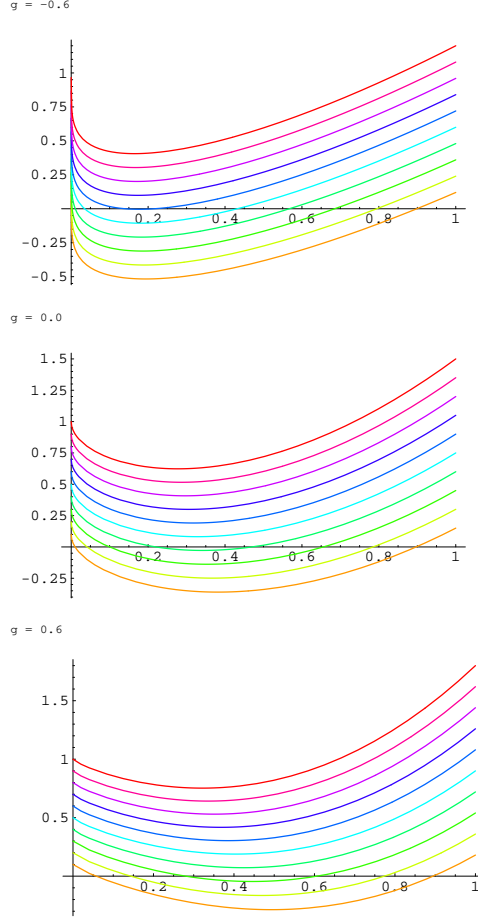


Figure 2: Sample plots for roots of the algebraic Eq. (53): from top to bottom, for $\gamma = -0.6, 0, 0.6$, respectively. The numerical value of Eq. (53) is plotted on the vertical axes, and X_0 along the horizontal axes. For a given graph (i.e. γ), each curve corresponds to a choice for Θ ; one sees that there is a critical value Θ_c , below which there are always two real positive roots.

singularity. Now, note that if Eq. (53)—and thus $V(X_0)$ —has (at least) two real positive roots, it follows that $(dV/dX_0) = f_0 - 1 < 0$ along one of the roots, and $f_0 - 1 > 0$ along the other. Hence, in such a case, there is a one-parameter family of ORNG leaving the singularity. A straightforward numerical analysis of the roots of Eq. (53), shows that for initial data in the shaded region (excluding its interface boundary; cf. Fig 1.), there are always two real positive roots (cf. Fig. 2).

Thus, we conclude that there are infinite number of ORNGs with past endpoint at the singularity.

5 Curvature strength

A defining property of the physical seriousness of a singularity is its curvature strength. A singularity is said to be gravitationally strong in the sense of Tipler [8] if every collapsing volume element is crushed to zero at the singularity, and weak otherwise (i.e., if it remains finite). It is generally believed—although not yet proven [30]—that spacetime is geodesically incomplete at a strong singularity, but extendible through a weak one [8, 31].

A precise characterization of Tipler strong singularities has been given by Clarke and Królak [32], who proposed (among other conditions) the *limiting strong focusing condition*: There is at least one non-spacelike geodesic, with tangent vector K^a and affine parameter λ (with $\lambda = 0$ at the singularity), along which the scalar $\Psi \equiv R_{ab}K^aK^b$ satisfies

$$\lim_{\lambda \rightarrow 0} \lambda^2 \Psi > 0. \quad (62)$$

This is a sufficient condition for the singularity to be Tipler strong and corresponds to the vanishing of any two-form (for null geodesics), or three-form (for timelike geodesics) defined along such a geodesic, at the singularity, due to unbounded curvature growth.

5.1 Null geodesics

Let us now consider an ORNG with tangent $K^a = (K^\tau, K^r, 0, 0)$, where $K^a = \frac{dx^a}{d\lambda}$, and

$$K^\tau \equiv \frac{F}{R} = R' K^r, \quad (63)$$

where F can be written as an explicit function of the affine parameter, $F = F(\lambda)$, obeying the differential equation (which follows from the geodesic equation, $K^a \nabla_a K^b = 0$):

$$\frac{dF}{d\lambda} + F^2 \left(\frac{\dot{R}'}{RR'} - \frac{\dot{R}}{R^2} - \frac{1}{R} \right) = 0. \quad (64)$$

In our case, we have

$$\begin{aligned} \Psi &= \frac{2m'}{R^2 R'} (K^\tau)^2 = \Theta^2 \left(\frac{r}{R} \right)^{1+\gamma} \frac{(K^\tau)^2}{R^2} \\ &= \Theta^2 X^{-5-\gamma} \frac{F^2}{r^4}, \end{aligned} \quad (65)$$

where Eqs. (47)-(48), and (64) were used. Hence,

$$\begin{aligned} \lim_{\lambda \rightarrow 0} \lambda^2 \Psi &= \Theta^2 X_0^{-5-\gamma} \lim_{\lambda \rightarrow 0} \frac{\lambda^2}{F^{-2} r^4} \\ &= \Theta^2 X_0^{-5-\gamma} \lim_{\lambda \rightarrow 0} \frac{1}{\Omega^2 r^4} \\ &= X_0^2, \end{aligned} \quad (66)$$

where l'Hôpital's rule was used twice, and [from Eq. (64)]

$$\Omega \equiv \frac{1}{Xr^2} \left(\Theta X^{-(5+\gamma)/2} - r \right). \quad (67)$$

Since $X_0 > 0$ always exists (cf. previous subsection), we conclude that the singularity is Tipler strong *independently* of the details of the initial data. We note, also, that there are infinite number of ORNGs with past endpoint at the singularity, each one of them defined by a unique tangent vector (on the $\{u, R\}$ plane) X_0 , which is determined from the initial data (C and γ). This constitutes a rather robust result, in that (i) the singularity is Tipler strong irrespective of the initial data, and (ii) it is so along an infinite number of ORNGs terminating at the singularity in the past.

5.2 Timelike geodesics

Let us consider radial timelike geodesics (RTGs), with tangent vector $\xi^a = \frac{dx^a}{d\lambda}$, where λ is proper time along the geodesic, and

$$\xi^\tau = \pm \sqrt{1 + R'^2 (\xi^r)^2}, \quad (68)$$

$$\xi^r R' + 2\xi^r \dot{R}' + \frac{\xi^r}{\xi^\tau} (\xi^r)' R' + \frac{(\xi^r)^2}{\xi^\tau} R'' = 0, \quad (69)$$

where the first equation is simply $\xi^a \xi_a = -1$, and the second follows from the geodesic equation. By inspection, one sees that Eq. (69) admits the trivial solution

$$\xi^\tau = \pm 1, \quad (70)$$

$$\xi^r = 0, \quad (71)$$

which leads to

$$\tau = \tau_i \pm (\lambda - \lambda_0), \quad (72)$$

$$r = r_0 = \text{const.}, \quad (73)$$

where the plus or minus sign refers to outgoing or ingoing RTGs, respectively. The outgoing RTG departing from the singularity is given by $r = 0$, and $\tau = \tau_0 + \lambda - \lambda_0$, and thus does not belong in the spacetime.

The ingoing RTG is given by $r = 0$, $\tau = \tau_0 - \lambda + \lambda_0$, where $\tau_i = \tau_0(0) = 0$ is the time at which the RTG arrives at the singularity. For this RTG, we have

$$\Psi \equiv R_{ab} \xi^a \xi^b = R_{\tau\tau} (\xi^\tau)^2 = \frac{m'}{R^2 R'} = 4\pi C \frac{r^{1+\gamma}}{R^{3+\gamma}}. \quad (74)$$

From Eqs. (33) and (72) we get

$$R = [Ar^{1+\gamma}(\lambda - \lambda_0)^2]^{\frac{1}{3+\gamma}}, \quad (75)$$

which gives

$$\Psi = \frac{2}{(\lambda - \lambda_0)^2(3 + \gamma)^2}. \quad (76)$$

Thus

$$\lim_{\lambda \rightarrow \lambda_0} (\lambda - \lambda_0)^2 \Psi = \frac{2}{(3 + \gamma)^2}. \quad (77)$$

Hence, the singularity is always Tipler strong along the RTG, irrespective of the initial data.

6 The dust limit

When $\gamma = 0$, we have, from Eqs. (33) and (29):

$$R(\tau, r) = \left(\frac{9m}{2}\right)^{\frac{1}{3}} (\tau_0 - \tau)^{\frac{2}{3}}, \quad (78)$$

where

$$m = m(r) = 4\pi Cr = 4\pi C\rho(0, r)r^3. \quad (79)$$

Equation (78) is exactly the same as the one in the marginally bound inhomogeneous dust case [28]. However, as can be seen from Eq. (79), the $\gamma = 0$ limit of our model is a particular case of the general inhomogeneous case. The initial mass function cannot be arbitrarily specified, with the only free parameter being the constant C .

At $\tau = \tau_0(r)$, a curvature singularity forms. Events with $r > 0$ are spacelike and thus covered (cf. Sec. III). Of potential interest is the $r = 0$ singularity. The visibility of such a singularity is determined by the existence of real positive roots of the algebraic equation (53). In this case, this equation reduces to the quartic:

$$P(Y) = Y^4 + \frac{\Theta}{2}Y^3 - Y + \Theta = 0, \quad (80)$$

where $Y \equiv \sqrt{X_0}$. Standard results from polynomial theory can be used to show that there is a maximum value $\Theta_{\max} = 0.425343$, above which all the roots of the quartic are complex. This result agrees with that of Joshi and Singh (JS) for pure dust [28], upon identification of the mass function in the two approaches, whence one finds [cf. Eqs. (13)-(15) in Ref. [28]]:

$$\Theta_{\max}^2 = 8\pi C = \lambda_{\text{JS}} = 16\beta_{\text{JS}} = 0.180917. \quad (81)$$

For $\Theta \in (0, \Theta_{\max}]$, there are two complex conjugate roots and two real positive-definite roots. (When $\Theta = 0$, we obtain the trivial solution $Y = X_0 = 0$ and $Y = X_0 = 1$, where the former is a degenerate case, where the tangent to the ORNG vanishes on the $\{u, X\}$ plane).

As an alternative way of showing the result above, note that Eq. (80) defines a two-dimensional surface that intersects the $P = 0$ plane along a curve $\Theta_0(Y)$, given by solving Eq. (80) for Θ :

$$\Theta_0(Y) = -2 \frac{Y(Y^3 - 1)}{Y^3 + 2}.$$

On the $P = 0$ plane, Θ_0 has an absolute maximum at $Y_* = 0.581029$, with $\Theta_0(Y_*) = 0.425343$.

From the results of Sec. V, we find that the central singularities in the pure dust limit are Tipler strong along an infinite number of ORNGs and at least one IRTG, irrespective of the initial data, in agreement with earlier results for general inhomogeneous dust [10].

7 Discussion and Conclusions

The spherical symmetric collapse of dust with non-vanishing radial pressure Π , and vanishing tangential stresses was studied. When restricted to marginally bound configurations ($k = 0$), the field equations were analytically integrated in closed form. The $k = 0$ ansatz, together with the equation of state $\Pi = \gamma\rho$, implies that the initial data consists of two free parameters, Θ and γ , which measure the “strength” of the initial density and pressure profiles, respectively.

As in the pressureless dust case, a central singularity forms, which is Tipler strong along an infinite number of ORNGs, and at least one IRTG. Even though, in the timelike case, curvature growth was studied along a particular geodesic, using similar causal structure arguments to those of Deshingkar, Joshi, and Dwivedi [10], we can qualitatively show the existence of an infinite number of IRTG with future endpoint at the singularity, as follows. The existence of a future-directed timelike geodesic $\sigma(\lambda)$ with future endpoint at the singularity (proved in Sec. V), implies that its chronological past $I^-[\sigma]$ is a *timelike indecomposable past set* (TIP) [33]. In other words, the TIP is generated by σ , which is timelike and future-inextendible. The locally naked singularity itself—which is the future endpoint of σ , $\sigma(\lambda_0)$ —constitutes a singular TIP which contains the past $I^-(p)$ of any point $p \in \sigma \setminus \{\sigma(\tau_0)\}$ [34]. Consider now another point $q \notin \sigma$ in the past of the singularity and in the chronological past of p . Since $I^-(q) \subset I^-(p)$, it follows that there exists a timelike curve from p to q , say ζ , satisfying $I^-[\zeta] \subset I^-[\sigma]$. Consider then a small compact ball \mathcal{B} —with a suitably defined “radius”, e.g., proper geodesic distance along σ , $d_\sigma(\lambda, \lambda_0)$ —in the neighborhood of $\sigma(\tau_0)$, partially contained in TIP $I^-[\sigma]$ and in the chronological future of p , i.e., $\mathcal{B} \cap I^-[\sigma] = \mathcal{C} \not\subset \emptyset$ and $I^+[\mathcal{C}] \subset I^+(p)$. For each point $x \in \mathcal{C}$, there is a timelike geodesic from p to x . Since \mathcal{C} is compact, there are infinite number of such points that can be joined by timelike geodesics from $p \in \sigma$. Now, let p be an arbitrary point on σ and take the limit of approach to the singularity, $d_\sigma(\lambda, \lambda_0) \rightarrow 0^+$; it then follows that there are infinite number

of future-inextendible timelike geodesics with future endpoint at the singularity.

More important than the directional behavior of curvature strength, is the visibility of the singularity. We found an infinite number of ORNGs with past endpoint at the singularity, which is therefore at least locally naked. The existence of such ORNGs is independent of the initial data. This differs from the pressureless inhomogeneous dust case, where the visibility of the central singularity depends crucially on differentiability properties of the central energy density distribution, and it is because our model reduces to a pressureless dust class with a particular mass function ($m \propto r$). In our model, the initial energy density distribution has a single degree of freedom (Θ), and is C^∞ everywhere except at the center, where it diverges as r^{-2} . However, the mass function is everywhere finite (it vanishes at $r = 0$), and the metric is everywhere regular. We remark that the divergence of the energy density at $r = 0$ does *not* preclude our model from being a useful test-bed for cosmic censorship. The issue of cosmic censorship is the issue of the development of singularities—signalled by the formation of trapped surfaces [1]—from an initial spacelike slice that does not admit trapped surfaces and on which the induced metric is regular, in the *causal future* of that slice. In our model, the initial data (Θ and γ) are such that the metric is *everywhere regular*, and there are no trapped surfaces on the initial slice. We have shown that, from a large subset of initial data, trapped surfaces—and, consequently, singularities—inevitably form in the causal future of such regular initial slices. Accordingly, whereas this model may not provide a realistic approximation for the central density, it constitutes a well-defined test-bed spacetime to examine the isolated effects of radial pressure on the formation and visibility of the central singularity.

We find that positive radial pressure tends to suppress visible singularities, and negative radial pressure tends to uncover them. Our negative pressure data space complements the results of Cooperstock *et al.* for non-central singularities [18], to include the $r = 0$ case. The most significant result is that, irrespective of the strength of the radial pressure, there is always a set of non-zero measure in the parameter space that leads to visible singularities. Hence, we find that radial pressure alone cannot eliminate the naked singularity spectrum. We conjecture that this behavior is not particular to our (marginally bound) model, and that it will exist in *any* spherical system with an equation of state of the form $\Pi = \gamma\rho$. In addition, since tangential stresses alone tend to uncover the singularity spectrum, and radial pressure by itself fails to fully cover it, we further speculate that when the former and latter are taken together into account, visible singularities will still persist.

In order to confidently establish the role of radial pressure and the combined roles of tangential and radial stresses in the final state of gravitational collapse, further analyses need to be undertaken, of non-marginally-bound systems, and explicitly including tangential stresses. Efforts in this direction are

currently underway [35].

Acknowledgments

The authors are grateful to P. Brady, T. Harada, H. Iguchi, P. Joshi, H. Kodama, and K. Thorne for helpful discussions and/or comments. SJ thanks T. Tanaka for help with producing Mathematica figures. SMCVG acknowledges the support of FCT (Portugal) Grant PRAXIS XXI-BPD-16301-98, and NSF Grant AST-9731698. SJ acknowledges the support by Grant-in-Aid for JSPS fellows (No. 00273).

References

- [1] S. W. Hawking and G. F. R. Ellis, *The Large Scale Structure of Space-Time* (Cambridge University Press, Cambridge, England, 1973).
- [2] R. Penrose, Riv. Nuovo Cimento **1**, 252 (1969).
- [3] R. Penrose, in *General Relativity, An Einstein Centenary Survey*, edited by S. W. Hawking and W. Israel (Cambridge University Press, Cambridge, 1979).
- [4] See, e.g., D. Christodoulou and S. Klainerman, *The Global Nonlinear Stability of Minkowski Space* (Princeton University Press, Princeton, 1993); A. D. Rendal, Ann. Phys. **233**, 82 (1994); B. K. Berger *et al.*, Mod. Phys. Lett. A **13**, 1565 (1998); L. Andersson, “The global existence problem in general relativity”, gr-qc/9911032.
- [5] G. Lemaître, Ann. Soc. Sci. Brussels **A53**, 85 (1933); R. C. Tolman, Proc. Nat. Acad. Sci. USA **20**, 410 (1934); H. Bondi, Mon. Not. Astron. Soc. **107**, 343 (1948).
- [6] D. M. Eardley and L. Smarr, Phys. Rev. D **19**, 2239 (1979); D. Christodoulou, Commun. Math. Phys. **93**, 171 (1984); R. P. A. C. Newman, Class. Quantum Grav. **3**, 527 (1986); P. S. Joshi and I. H. Dwivedi, Commun. Math. Phys. **146**, 333 (1992); I. H. Dwivedi and P. S. Joshi, Class. Quantum Grav. **9**, L69 (1992); K. Lake, Phys. Rev. Lett. **68**, 3129 (1992); P. S. Joshi and I. H. Dwivedi, Phys. Rev. D **47**, 5357 (1993); T. P. Singh and P. S. Joshi, Class. Quantum Grav. **13**, 559 (1996); S. Jhingan, P. S. Joshi, and T. P. Singh, Class. Quantum Grav. **13**, 3057 (1996); S. S. Deshingkar, P. S. Joshi, and I. H. Dwivedi, Phys. Rev. D **59**, 044018 (1999).
- [7] The results for asymptotically dust collapse have recently been generalized to include a cosmological constant, with similar conclusions. See S. M. C. V. Gonçalves, Phys. Rev. D **63**, 064017 (2001); S.

- S. Deshingkar, S. Jhingan, A. Chamorro, and P. S. Joshi, “Gravitational collapse and cosmological constant”, to appear in Phys. Rev. D, gr-qc/0010027.
- [8] F. J. Tipler, Phys. Lett. **64A**, 8 (1977).
- [9] S. Jhingan and P. S. Joshi, in *Internal Structure of Black Holes and Spacetime Singularities*, Vol. **XIII** of the Annals of the Israel Physical Society, edited by L. M. Burko and A. Ori (IOP, Bristol, England, 1997).
- [10] S. S. Deshingkar, P. S. Joshi, and I. H. Dwivedi, in Ref. [6] above. See also T. P. Singh, Phys. Rev. D **58**, 108502 (1998).
- [11] T. Harada, H. Iguchi, and K. Nakao, Phys. Rev. D **58**, 041502 (1998); H. Iguchi, T. Harada, and Nakao, Prog. Theor. Phys. **101**, 1235 (1999); **103**, 53 (2000).
- [12] T. Nakamura and H. Sato, Prog. Theor. Phys. **67**, 346 (1982).
- [13] See, e.g., J. C. Miller and D. W. Sciama, in *General Relativity and Gravitation*, edited by A. Held (Plenum, New York, 1980), Vol. 2.
- [14] P. S. Joshi and I. H. Dwivedi (1992), in Ref. [6] above; Lett. Math. Phys. **27**, 235 (1993).
- [15] B. J. Carr and A. A. Coley, Phys. Rev. D **62**, 044023 (2000).
- [16] J. F. V. Rocha, A. Wang, and N. O. Santos, Phys. Lett. **255A**, 213 (1999).
- [17] See, e.g., M. A. Podurets, Sov. Phys.-Dokl. **11**, 275 (1966).
- [18] F. I. Cooperstock, S. Jhingan, P. S. Joshi, and T. P. Singh, Class. Quantum Grav. **14**, 2195 (1997).
- [19] A. Ori and T. Piran, Phys. Rev. Lett. **59**, 2137 (1987); Phys. Rev. D **42**, 1068 (1990).
- [20] T. Harada, Phys. Rev. D **58**, 104015 (1998).
- [21] I. H. Dwivedi and P. S. Joshi, Commun. Math. Phys. **166**, 117 (1994). See also K. Lake in Ref. [6] above.
- [22] Consider a 2-dimensional subspace of the tangent space of an arbitrary point in the spacetime, which is mapped to itself by the Ricci tensor R^a_b . Depending on the number and norm of the eigenvectors of this invariant 2-plane, the Ricci tensor—and hence the stress-energy tensor—can be classified into four different types. Type I matter is characterized by two real orthogonal eigenvectors, and includes most of the known physical descriptions of matter: electromagnetic field,

- perfect fluid, and dust (with or without a Λ -term). In spherical symmetry, these matter fields are described by a diagonal stress-energy tensor, in comoving coordinates. For further details see D. Kramer, H. Stephani, E. Herlt, and M. MacCallum, *Exact Solutions of Einstein's Field Equations* (Cambridge University Press, Cambridge, England, 1980).
- [23] G. Magli, *Class. Quantum Grav.* **14**, 1937 (1997); **15**, 3215 (1998); T. Harada, H. Iguchi, and K. Nakao, in Ref. [11] above; S. Jhingan and G. Magli, *Phys. Rev. D* **61**, 124006 (2000).
 - [24] S. Jhingan and G. Magli, in *General Relativity*, edited by D. Fortunato, A. Masiello, B. Casciaro, and M. Francaviglia (Springer-Verlag, Berlin/Heidelberg, 1999), gr-qc/9903103.
 - [25] C. W. Misner and D. H. Sharp, *Phys. Rev. B* **136**, 571 (1964).
 - [26] K. S. Thorne, “Numerical Relativity for Inspiring Binaries in Co-Rotating Coordinates: Test Bed for Lapse and Shift Equations”, gr-qc/9808024.
 - [27] G. Darmon, *Mémoires des Sciences Mathématiques* **25** (Gauthier-Villars, Paris, France, 1927); W. Israel, *Riv. Nuovo Cimento* **44B**, 1 (1966).
 - [28] P. S. Joshi and T. P. Singh, *Phys. Rev. D* **51**, 6778 (1995).
 - [29] P. S. Joshi and I. H. Dwivedi (1993), in Ref. [6] above.
 - [30] C. J. S. Clarke, *Analysis of Spacetime Singularities* (Cambridge University Press, Cambridge, England, 1993).
 - [31] F. J. Tipler, C. J. S. Clarke, and G. F. R. Ellis, in *General Relativity and Gravitation*, edited by A. Held (Plenum, New York, 1980), Vol. 2; A. Ori, *Phys. Rev. Lett.* **67**, 789 (1992).
 - [32] C. J. S. Clarke and A. Królak, *J. Geom. Phys.* **2**, 127 (1985).
 - [33] R. Geroch, E. H. Kronheimer, and R. Penrose, *Proc. R. Soc. Lond.* **A327**, 545 (1972).
 - [34] R. Penrose, in *Theoretical Principles in Astrophysics and Relativity*, edited by N. R. Liebowitz, W. H. Reid, and P. O. Vandervoort (Chicago University Press, Chicago, 1978).
 - [35] S. M. C. V. Gonçalves and S. Jhingan (in preparation).